ACS APPLIED MATERIALS & INTERFACES

Research Article

www.acsami.org

Improved Transfer Quality of CVD-Grown Graphene by Ultrasonic Processing of Target Substrates: Applications for Ultra-fast Laser Photonics

Guanpeng Zheng,[†] Yu Chen,[†] Huihui Huang,*[,‡] Chujun Zhao,[†] Shunbin Lu,[†] Shuqing Chen,[†] Han Zhang,*[,†] and Shuangchun Wen[†]

[†]Key Laboratory for Micro-/Nano-Optoelectronic Devices of Ministry of Education, College of Physics and Microelectronic Science, Hunan University, Changsha 410082, P. R. China

[‡]College of Optoelectronic Engineering, Shenzhen University, Shenzhen 518060, P. R. China

Supporting Information

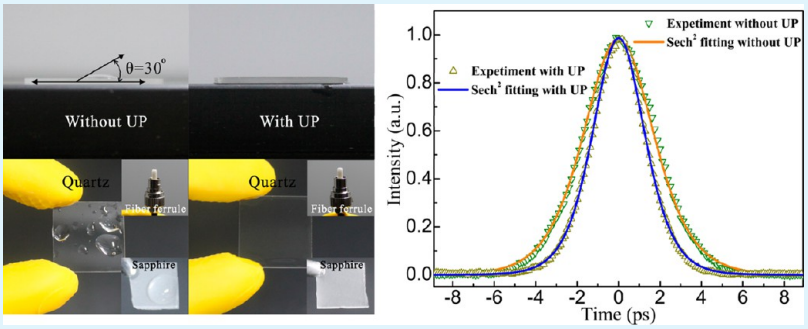

ABSTRACT: In this paper, we experimentally found that the transfer quality of CVD-grown graphene could be improved by ultrasonic processing (UP) of target substrates thanks to the improved hydrophilicity. Atomic force micrograph and Raman spectroscopy revealed that the graphene films transferred onto the target substrate with UP possess less wrinkles and defects than that of the sample without UP. The improvement technique endows graphene more suitable for photonics applications because of its weaker optical loss, higher optical damage threshold and longer stability. By integrating a fiber pigtailed graphene (treated by UP) device into a fiber laser cavity, we could obtain narrower mode-locked pulse with higher optical-to-optical conversion efficiency and better optical spectral profile, in contrast with that without UP, which further verify the improved transfer quality of graphene by the UP technique. We anticipate that this transfer technique may be applicable to boost the performance of other graphene photonics devices, such as optical modulator, detector, polarizer, etc.

KEYWORDS: *graphene, ultrasonic processing, hydrophilicity, graphene transfer, wrinkles, mode-locked fiber laser*

1. INTRODUCTION

Graphene, a two-dimensional (2D) material,[1] has been considered as a promising material for electronic devices due to its exceptional electronic transport properties.[2−7] Besides, its photonic properties are equally remarkable,[8−11] which enables graphene as an efficient saturable absorber for the generation of ultra-short pulse.[12−14] Unlike traditional saturable absorbers, such as single-walled carbon nanotubes, graphene saturable absorber (GSA) possesses many advantages, such as large and tunable modulation depth, low saturable absorption threshold and wavelength independent saturable absorption property.[15−17] To fabricate these devices with advanced performance, the search for a reliable transfer technique of high-quality graphene onto target substrates like optical fiber-ferrules or optical quartz substrate is always highly encouraged.

Among all the fabrication techniques of graphene, chemical vapor deposition (CVD) is commonly regarded as a low cost and scalable technique to obtain large-area, high-quality, and uniform graphene films.[18−21] Concerning the CVD-grown graphene, wet transfer, such as polymethylmethacrylate (PMMA) transfer method,[22] is typically employed. However, wrinkles or cracks always emerge together with the process of transferring graphene,[18,21−24] which may degrade its operation performance. This issue becomes more problematic for the graphene photonics devices, particularly in that wrinkles or cracks can introduce unwanted optical scattering loss that will consume more energy and weaken the output light intensity, as well as generate heat dissipation problem that can result in the optical damage of the device and therefore further limit its operation towards the high power regime. It has been reported that the increase in hydrophilicity of the target substrates where graphene samples are attached could significantly suppress the formation of

Received: August 2, 2013
Accepted: October 1, 2013
Published: October 1, 2013

large folds and wrinkles.[24] On basis of this, techniques that can increase the hydrophilicity of the target substrate had been widely developed.[24,25] However, most of those methods are complex, high-cost, environmentally unfriendly (e.g. using strong acid to enhance the hydrophilicity) or incompatible with some substrates like fiber-ferrules.

In this paper, we present a simple approach to improve the hydrophilicity of the target substrates by ultrasonic processing (UP) in deionized (DI) water. Ultrasonic is considered as a "green" technology because of its high efficiency, economic performance and low level of facility requirement.[26−28] We found that UP can significantly increase the hydrophilicity of the target substrate, rendering the transferred graphene with higher quality and less wrinkles and defects. More importantly, we also experimentally noted that the UP technique is also widely applicable for other substrates, such as sapphire, optical fiber. Upon ultrasonic processing the end-facet of the optical fiber where graphene film is attached yields a high performance graphene SA optical device, which can be further incorporated into an erbium-doped fiber laser for better mode-locking performance, suggesting the effectiveness of the UP technique in improving the performance of graphene optical devices.

2. EXPERIMENTAL SECTION

2.1. Preparation of Target Substrates. Two sets of fresh quartz/sapphire substrates and two pieces of optical fiber ferrules were prepared with a standard wet cleaning procedure and followed by drying in an oven. To study the influence of ultrasonic to the surface of target substrate, one set of the cleaned quartz/sapphire substrates and one piece of optical fiber ferrules were ultrasonic processed in DI water for 20 minutes while the left substrates/fiber ferrules were kept untreated. UP of substrates/fiber ferrules was carried out in an ultrasonic bath (KQ-300DE, Kun Shan Ultrasonic Instruments Co., Ltd, China) with ultrasonic frequency and power of 40 kHz and 300 W, respectively.

2.2. Transfer of Graphene Films. CVD-grown graphene (ACS MATERIAL LLC, Grown on Cu, 5 cm ×5 cm, 6-8 layers) films were transferred to target substrates with the widely-used PMMA transfer method.[22] As partially illustrated in Figure 1, the typical procedure includes: (1) the graphene-on-metal substrates were spin coated with a thin layer of PMMA (Micro Chem. 950 K, 5 wt % in acetone), followed by baking at 100 °C for 10 min; (2) the PMMA-capped graphene was then put into a $FeCl_3$ (2M) solution to completely etch off the underlying copper film; (3) the PMMA-capped graphene film was then transferred to DI water to remove the etchant and residues; (4) the target substrate (quartz or fiber ferrule) was then used to "fish out" the PMMA-capped graphene film, followed by drying in an oven for 5 minutes at 70 °C to dehydrate the substrates, thereby improving the adhesion of PMMA-capped graphene film to the substrates; (5) the samples were placed in acetone to lift off the PMMA, followed by baking at 100 °C for 3−5 minutes to remove the solvent.

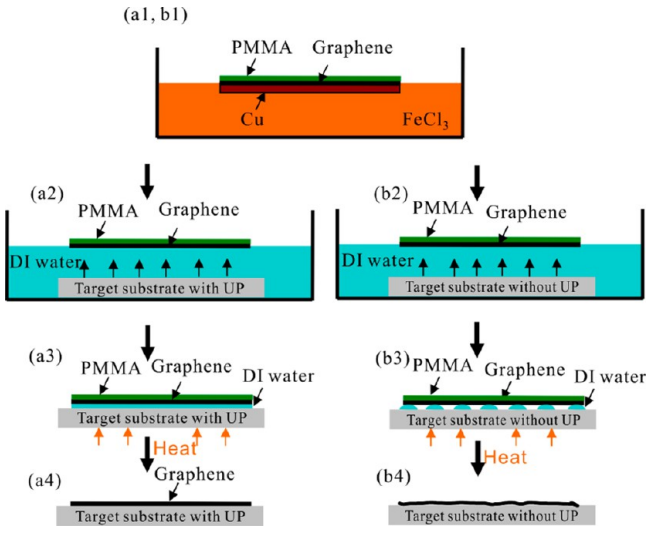

Figure 1. Schematic illustration of the transfer processes. Graphene films were transferred onto (a) target substrate with UP and (b) target substrate without UP.

2.3. Design of the Graphene SA-Based Mode-Locked Fiber Laser. To construct a passively mode-locking ring laser cavity, the experimental configuration as in Figure 6 was employed, including the standard fiber-optic components such as wavelength division multiplexer (WDM), polarization controller (PC), coupler, optical isolator, erbium-doped fiber (EDF), and single mode fiber (SMF). The fiber laser operating in the anomalous dispersion regime has a ring cavity configuration with a total cavity length of 57.4 m, which comprises a piece of 1 m erbium-doped fiber (EDF, LIEKKI Er 80-8/125) with group velocity dispersion (GVD) of −20 ps^2/km and 56.4 m standard single mode fiber (SMF-28) with GVD of −23 ps^2/km at 1550 nm. The pump from a 975 nm laser diode (LD) source is coupled into the cavity through a 980/1550 wavelength-division multiplexer (WDM), and a 10% fiber coupler is employed to output the in-cavity light. A polarization independent isolator (PI-ISO) is used to force the unidirectional operation of the ring cavity, and a polarization controller (PC) is used to fine adjust the polarization state of circulating light and the in-cavity birefringence. An optical spectrum analyzer (Ando AQ-6317B) and an oscilloscope (Tektronix TDS3054B) combined with a 5 GHz photo-detector (Thorlabs SIR5) are employed to simultaneously monitor the optical spectra and temporal profile of the output pulse train. The pulse duration is measured by a commercial second harmonic generation auto-correlator.

2.4. Characterization. Atomic force microscope (AFM) measurements were carried out in a SPM-9500J3 system. Raman spectra were obtained by a Labram-010 system. Laser spot images were captured by a Coherent Laser Cam-HRTM Beamview system (1280 × 1024 pixels, pixel size 6.7 μm).

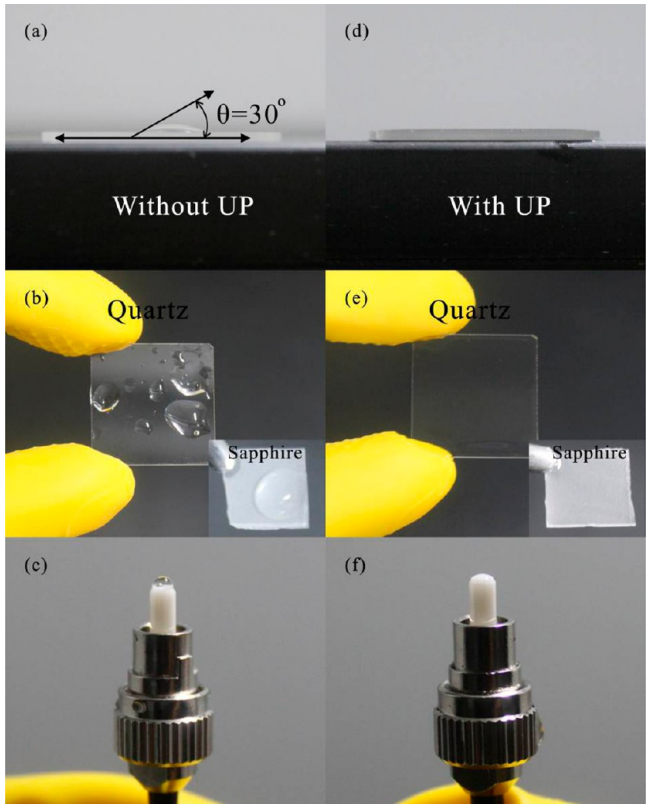

Figure 2. Photographic images of the DI water droplets on the target substrates: (a, b, c) substrates without UP and (d, e, f) substrates with UP.

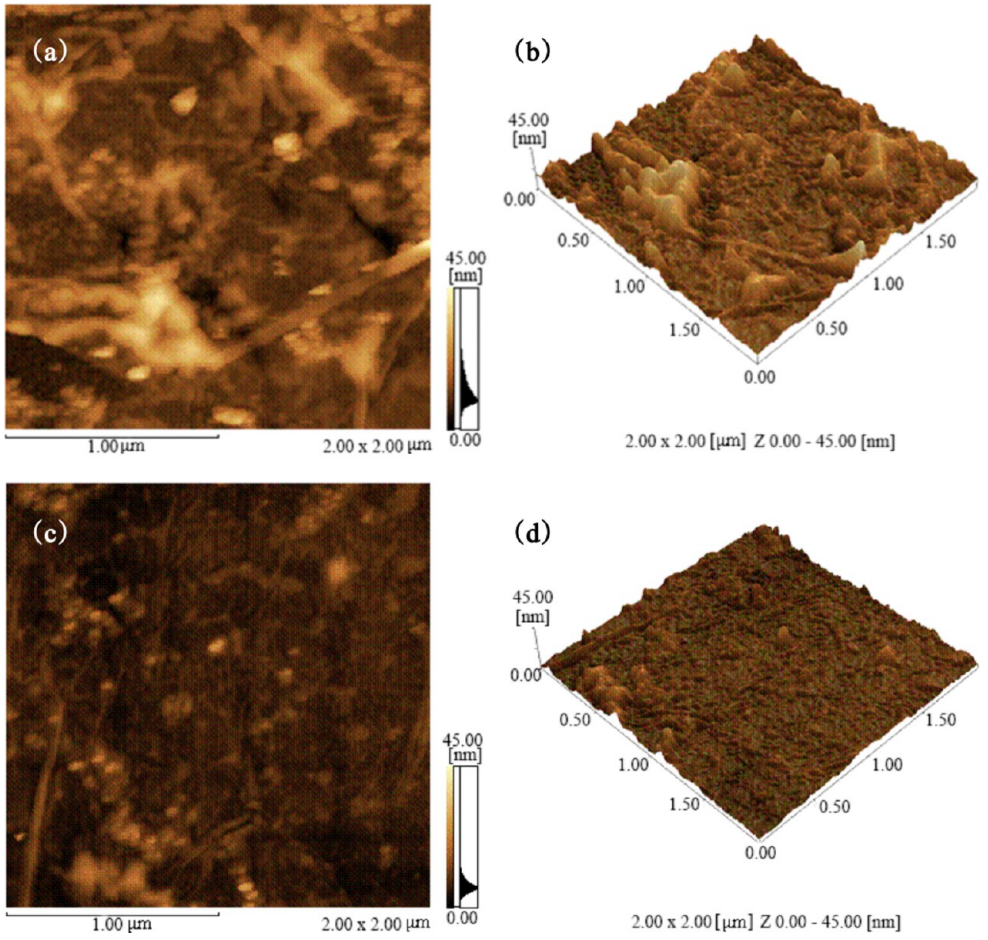

Figure 3. AFM images of graphene films on the quartzs: (a, b) without UP and (c, d) with UP. (a, c) 2D images and (b, d) 3D images.

3. RESULTS AND DISCUSSION

Figure 2 compares the wettability of the target substrates without and with UP. In the following, after rinsing with DI water, the shapes of the DI water droplets deposited on the optical quartz substrates (without and with UP) were compared in Figure 2a and 2d, respectively. It could be seen that water droplet settled on the quartz with UP was completely dispersed, whereas an obvious droplet with a contact angle of ~30° appeared on the quartz without UP (see Figure 2a). Besides, the water droplets on the quartz substrates without UP were kept as an irregular shape (see Figure 2b), whereas a uniform water film was formed on the surface of the quartz with UP (see Figure 2e), similar results could be observed for the water droplets on the sapphire (see the insets of Figure 2b and 2e) and fiber ferrule (see Figure 2c and 2f). According to Young's equation,[29] the hydrophilicity of a surface can be gauged by measuring the contact angle (θ, see Figure 2a) of a droplet of water on the surface. The smaller the contact angle is, the higher hydrophilicity of the substrate can be deduced. Therefore, the above results proved that the hydrophilicity of various substrates including quartz, sapphire, and fiber-ferrule could be significantly improved by UP technique, which also suggested that this method has a wider applicability for the graphene transfer technology. To understand the mechanism on modifying the substrate wettability by UP, surface properties of the quartz samples without and with UP were compared in terms of X-ray photoelectron spectroscopy (XPS) and AFM results, which revealed that the mechanism is not only attributed to the removal of hydrophobic "adventitious" carbon but also related with the much smoother surface at the condition with UP.[30] Details of which are shown in the Supporting Information.

To figure out the impact of the hydrophilicity of target substrates on the surface topography of transferred graphene films, the AFM images of graphene films transferred on the quartz substrates without UP and with UP were compared in Figure 3. One can obviously see that there is a significant

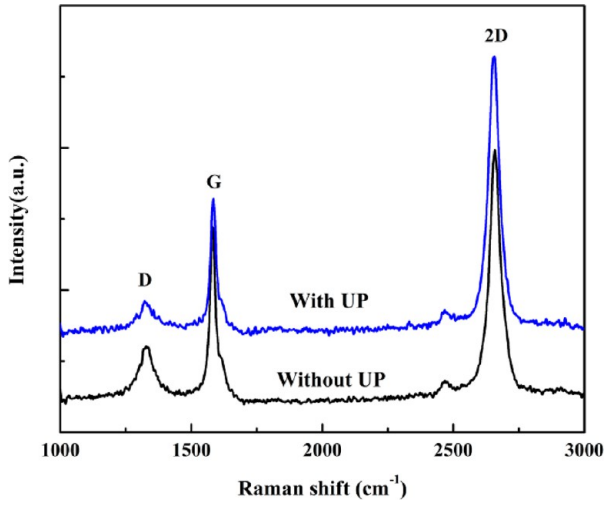

Figure 4. Raman spectra of graphene on quartzs with UP (blue) and without UP (black).

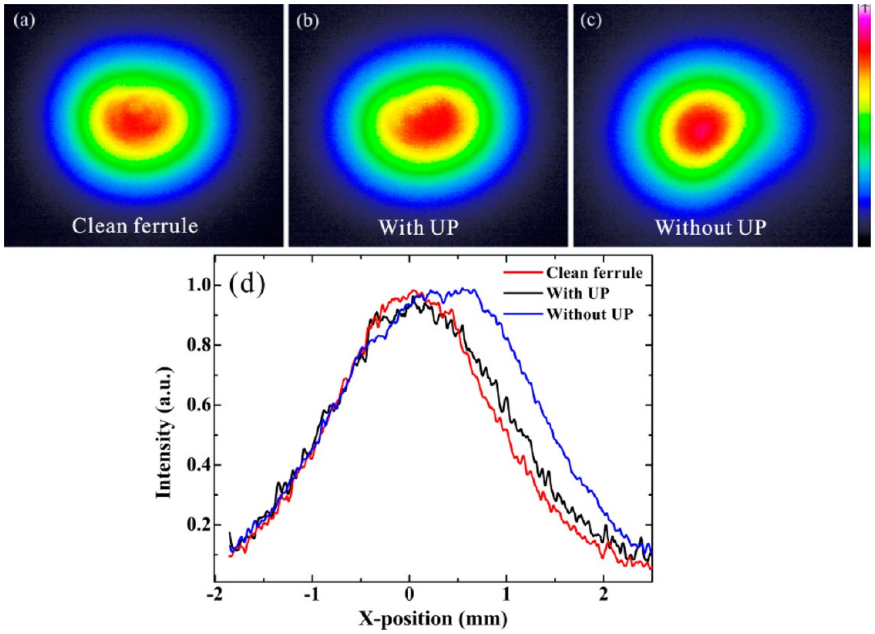

Figure 5. Spot profiles with CCD: Intensity distribution propagating after (a) clean ferrule, (b) sample with UP and (c) without UP, and (d) the corresponding cross line (y = 0).

difference between the two sets of AFM images under the same coordinates. The transferred graphene on the quartz with UP has much less cracks and corrugations (see Figure 3c and 3d) compared with those of the graphene on the quartz without UP (see Figure 3a and 3b). The reason could be tracked back to the transfer processes of the two types of target substrates, as illustrated in Figure 1. During the transfer process, when the PMMA/graphene stack is transferred from DI water to the target substrate, some water molecules retain between the PMMA/graphene film and the target substrate. With the drying and evaporation of the DI water between the graphene film and the substrate, the water surface tension will drag the graphene film to contact with the substrate.[24] If the surface of target substrate is hydrophilic (substrate with UP), the water between the substrate and the PMMA/graphene will spread more uniformly. Once the sample is baked, the contact between the graphene and the substrate is improved, which avoids the formation of large folds and cracks. However, if the substrate is not sufficiently hydrophilic (substrate without UP, for example), the water film between the graphene and substrate will break into droplets. After removing the droplets, the transferred graphene was unable to flatly lie upon the surface of the substrate, leading to the formation of small bubbles between the film and the substrate. Moreover, the imperfect contact between graphene and the substrate causes cracks and wrinkles after the PMMA is removed with acetone.

By further comparing the Raman spectra of graphene films transferred onto the quartz substrates with and without UP, one can verify the effectiveness of the UP technique. The quality of graphene can be quantified by analyzing the intensity ratio between the disorder-induced D band and the Raman-allowed G band (I_D/I_G).[31] Higher I_D/I_G value indicates more defects in graphene. The I_D/I_G value is calculated to be 0.184 for the graphene transferred on the quartz with UP, which is smaller than the value for the graphene on the quartz without UP (I_D/I_G = 0.265), implying that the graphene transferred on the quartz with UP has less defects than that of the sample without UP.

To make the graphene compatible with the fiber laser cavity, one can transfer graphene film onto FC/PC fiber ferrules with SMF pigtail which can be easily spliced inside the fiber laser cavity. Correspondingly, fiber graphene SA devices can be fabricated under two different conditions: with UP; without UP. By connecting these graphene-on-fiber components with another clean and dry FC/PC fiber connector, the GSA devices were thereby constructed for fiber laser application. Firstly, we measured the total insertion loss of the GSA devices with continuous wave at 1550 nm, which is about 0.82 dB and 0.91 dB for with UP and without UP, respectively.

Although we are unable to perform an in-situ AFM on those graphene fiber devices to find out whether graphene film on the optical fiber end-facet shows improved quality, an alternative measurement technique based on the beam propagation after passing through the graphene fiber devices can be employed to verify whether beam distortion can be suppressed by the UP technique. We recorded and compared the laser spot images of these two samples at the same distance of 1.5 cm with a high resolution CCD under the same illumination source (central wavelength 975 nm, continuous wave), as shown in Figure 5. At the condition with UP, the beam intensity profile after propagating through the sample is almost the same as the incident beam. However, at the condition without UP, the beam spot encountered moderate distortion in contrast with Figure 5a (after passing through a clean ferrule). This is because of the non-homogenous sample surface can disrupt the beam propagation from its original path and therefore decrease the coupling efficiency from one side of the SMF into another SMF. Such a difference can be further quantified by the beam intensity profile as shown in Figure 5d. At the condition with UP, the beam spot showing ideal Gaussian profile for the fundamental mode HE_{11} is almost identical with the incident beam profile. However, at the condition without UP, the beam distortion could be clearly seen since that the central parts were not coincident any longer. These differences are also related to the different roughness between the two types of transferred graphene (see Figure 3). It therefore accounts for the larger optical loss for the condition without UP.

Then, these devices were incorporated into an Erbium-doped fiber laser cavity as the passive mode-locker components. Figure 6 shows the experimental setup of the fiber laser. The basic operation of the laser is described in the Experimental Section. The ring cavity fiber laser could self-start the mode locking operation once the pump power was increased up to 52 mW at the condition with UP and 67 mW at the condition without UP. Figure 7a shows output power versus input power of our fiber laser, as can be seen, the slope at the condition with UP (1.84%) is higher than at the condition without UP (1.3%), indicating that UP can increase the optical-to-optical conversion efficiency. Figure 7b–7d describes the characteristics of single soliton pulse emitted from our fiber laser at the condition with UP and without UP while the other experiment conditions (like pump power of 81 mW, cavity setup, environmental perturbation, and so on) were kept the same. Figure 7b shows the single pulse train in temporal domain of with UP, in which, the fundamental repetition is about 3.59 MHz, corresponding to a cavity round trip time of about 279 ns that matches well with the total cavity length of 57.4 m, indicating that the fiber ring laser operates in the mode-locking state. The insert shows a long time scale of output pulse train, from which we could see the excellent long term stability of the output pulse without any modulation. However, at the condition without UP, once the pump power exceeds the mode-locking threshold, the multi-pulse instead of single pulse can be obtained no matter how the orientation of PC is adjusted. To confirm this soliton operating state, we also measured its corresponding spectra (see Figure 7c). Clear Kelly sidebands emerge in both spectra of with UP and without UP, which is a typical characteristic of soliton state in the anomalous dispersion cavity, showing that at both conditions the fiber laser operates in the soliton regime. It is worthwhile to note that with UP (resp. without UP) has a central wavelength of 1567.9 nm (resp. 1564.85 nm) and a 3 dB bandwidth of 1.35 nm (resp. 1.11 nm). We believe that the relatively larger loss of sample at the condition without UP leads to the central wavelength shifting towards the shorter wavelength. And also, we measured its output average power, which is 1.78 and 1.34 mW at the condition with UP and without UP respectively that further confirms the relatively larger loss of the condition without UP. Most importantly, at the condition without UP, the spectrum has strong continuous wave (CW), which introduces large additional perturbation on the mode-locking pulses and weakens the property for mode-locking, attributing to the relatively inferior quality of the sample at the condition without UP.[32] Figure 7d shows its autocorrelation trace. With UP has a full width at half maximum (FWHM) of about 2.962 ps, indicating that the real pulse width is 1.92 ps fitted by hyperbolic secant function. And the pulse duration of without UP is 2.58 ps. The time-bandwidth product at with UP and without UP is 0.316 and 0.351 respectively indicating that the obtained soliton pulses at both conditions are quasi-transform-limited pulses with slight chirp while the optical pulse at the condition without UP has larger chirp. All the above results verify that the graphene transferred onto target substrates with UP show higher-performance (such as higher output power, higher optical conversion efficiency,

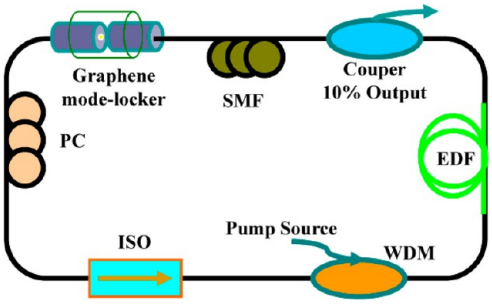

Figure 6. Schematic of the fiber ring laser. EDF: erbium-doped fiber. SMF: single-mode fiber. PC: poloarization controller. ISO: isolator. WDM: wavelength division multiplexer.

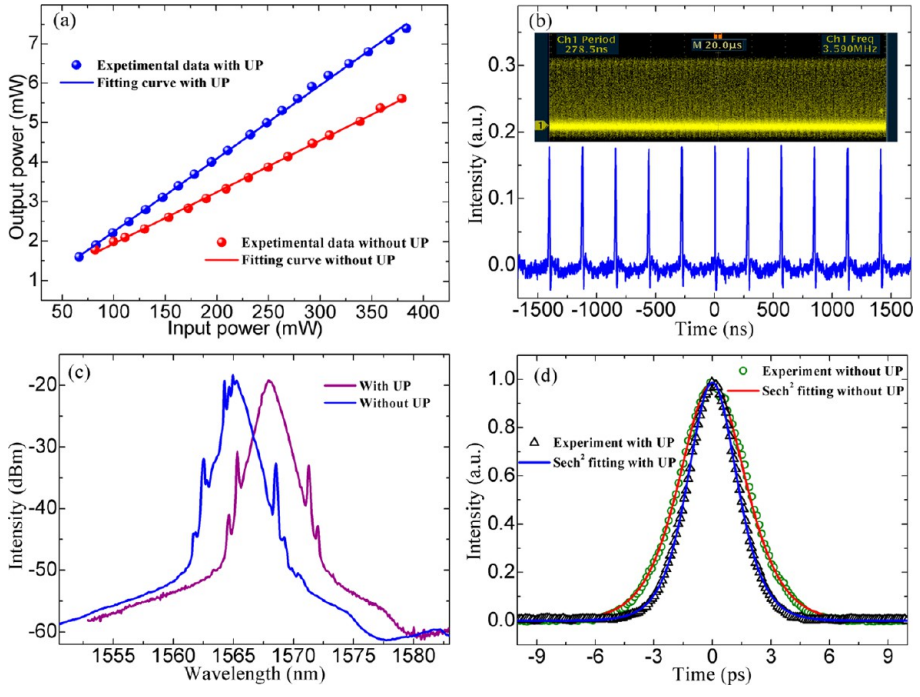

Figure 7. (a) Output power versus input power and soliton emitted from our fiber laser at pump power of 81 mW at the condition with UP and without UP. (b) Output single pulse train at the condition with UP. (c) Output spectra at the condition with UP and without UP. (d) Corresponding autocorrelation trace and its hyperbolic secant function fitting curve at the condition with UP and without UP.

narrower pulse duration and smoother spectral profile) as saturable absorbers that make them suitable for the ultra-fast fiber laser applications.

4. CONCLUSION

In summary, we proposed a simple and effective method to improve the transfer quality of graphene by UP of the target substrates, benefiting from the enhanced hydrophilicity. The corresponding AFM, Raman, and beam propagation spectra revealed that the graphene films transferred onto the target substrates with UP have less folds and defects than that of the graphene transferred on target substrates without UP, making graphene more favorable for photonic device with advantages of low optical loss, high optical damage threshold and stability. By comparing the mode-locker devices based on the different types of transferred graphene films, one can note that the performance of GSA in laser applications had been largely improved with UP technique, in terms of narrower pulse duration, higher conversion efficiency and smoother optical spectral profile. This simple, low-cost and widely compatible graphene transfer method should have great potential application values in various photonics fields.

■ ASSOCIATED CONTENT

Ⓢ Supporting Information

Mechanism of changing substrate wettability by UP is discussed in the text. This material is available free of charge via the Internet at http://pubs.acs.org/.

■ AUTHOR INFORMATION

Corresponding Authors

*E-mail: huang_huihui@foxmail.com.
*E-mail: hanzhang@hnu.edu.cn.

Author Contributions

G.Z. amd Y.C. contributed equally to this work.

Notes

The authors declare no competing financial interest.

■ ACKNOWLEDGMENTS

This work is partially supported by the National 973 Program of China (Grant No. 2012CB315701), the National 863 Program of China (Grant No. 2011AA010203). H.Z. acknowledges the support from Program for "Thousand Talents Program" for Distinguished Young Scholars and National Natural Science Fund Foundation of China for Excellent Young Scholars (Grant No. 61222505).

■ REFERENCES

(1) Katsnelson, M. I. *Mater. Today.* **2007**, *10*, 20−27.
(2) Ha, T. J.; Lee, J.; Chowdhury, S. F; Akinwande, D.; Rossky, P. J.; Dodabalapur, A. *ACS Appl. Mater. Interfaces* **2013**, *5*, 16−20.
(3) Lemaitre, M. G.; Donoghue, E. P.; McCarthy, M. A.; Liu, B.; Tongay, S.; Gila, B.; Kumar, P.; Singh, R. K.; Appleton, B. R.; Rinzler, A. G. *ACS Nano* **2012**, *6*, 9095−9102.
(4) Kim, S.; Nah, J.; Jo, I.; Shahrjerdi, D.; Colombo, L.; Yao, Z.; Tutuc, E.; Banerjee, S. K. *Appl. Phys. Lett.* **2009**, *94*, No. 062107.
(5) Lemme, M. C.; Echtermeyer, T. J.; Baus, M.; Szafranek, B. N.; Bolten, J.; Schmidt, M.; Wahlbrink, T.; Kurz, H. *Solid-State Electron.* **2008**, *52*, 514−518.
(6) Novoselov, K. S.; Geim, A. K.; Morozov, S. V.; Jiang, D.; Zhang, Y.; Dubonos, S. V.; Grigorieva, I. V.; Firsov, A. A. *Science* **2004**, *306*, 666−669.
(7) Neto, A. H. C.; Guinea, F.; Peres, N. M. R.; Novoselov, K. S.; Geim, A. K. *Rev. Mod. Phys.* **2009**, *81*, 109−162.
(8) Bao, Q.; Zhang, H.; Wang, B.; Ni, Z.; Lim, C.; Wang, Y.; Tang, D.; Loh, K. P. *Nat. Photonics* **2011**, *5*, 411−415.
(9) Bonaccorso, F.; Sun, Z.; Hasan, T.; Ferrari, A. C. *Nat. Photonics* **2010**, *4*, 611−622.
(10) Loh, K. P.; Bao, Q.; Eda, G.; Chhowalla, M. *Nat. Chem.* **2010**, *2*, 1015−1024.
(11) Zheng, Z. W.; Zhao, C. J.; Lu, S. B.; Chen, Y.; Li, Y.; Zhang, H.; Wen, S. C. *Opt. Express* **2012**, *20*, 23201−23214.
(12) Bao, Q. L.; Zhang, H.; Ni, Z. H.; Wang, Y.; Polavarapu, L.; Shen, Z. X.; Xu, Q. H.; Tang, D. Y.; Loh, K. P. *Nano Res.* **2011**, *4*, 297−307.
(13) Sun, Z. P.; Hasan, T.; Torrisi, F.; Popa, D.; Privitera, G.; Wang, F. Q.; Bonaccorso, F.; Basko, D. M.; Ferrari, A. C. *ACS Nano* **2010**, *4*, 803−810.
(14) Bao, Q. L.; Zhang, H.; Wang, Y.; Ni, Z. H.; Yan, Y. L.; Shen, Z. X.; Xu, Q. H.; Loh, K. P.; Tang, D. Y. *Adv. Funct. Mater.* **2009**, *19*, 3077−3083.
(15) Zhang, H.; Tang, D. Y.; Knize, R. J.; Zhao, L. M.; Bao, Q. L.; Loh, K. P. *Appl. Phys. Lett.* **2010**, *96*, No. 111112.
(16) Wang, Y. G.; Chen, H. R.; Wen, X. M.; Hsieh, W. F.; Tang, J. *Nanotechnology* **2011**, *22*, 455203.
(17) Liu, J.; Wang, Y. G.; Qu, Z. S.; Zheng, L. H.; Su, L. B.; Xu, J. *Laser Phys. Lett.* **2012**, *9*, 15−19.
(18) Li, X. S.; Cai, W. W.; An, J. H.; Kim, S.; Nah, J.; Yang, D. X.; Piner, R.; Velamakanni, A.; Jung, I.; Tutuc, E.; Banerjee, S. K.; Colombo, L.; Ruoff, R. S. *Science* **2009**, *324*, 1312−1314.
(19) Ren, W. C.; Gao, L. B.; Ma, L. P.; Cheng, H. M. *New Carbon Mater.* **2011**, *26*, 71−80.
(20) Juang, Z. Y.; Wu, C. Y.; Lu, A.; Su, C. Y.; Leou, K. C.; Chen, F. R.; Tsai, C. H. *Carbon* **2010**, *48*, 3169−3174.
(21) Reina, A.; Jia, X. T.; Ho, J.; Nezich, D.; Son, H. B.; Bulovic, V.; Dresselhaus, M. S.; Kong, J. *Nano Lett.* **2009**, *9*, 30−35.
(22) Li, X. S.; Zhu, Y. W.; Cai, W. W.; Borysiak, M.; Han, B. Y.; Chen, D.; Piner, R. D.; Colombo, L.; Ruoff, R. S. *Nano Lett.* **2009**, *9*, 4359−4363.
(23) Liu, N.; Pan, Z. H.; Fu, L.; Zhang, C. H.; Dai, B. Y.; Liu, Z. F. *Nano Res.* **2011**, *4*, 996−1004.
(24) Liang, X.; Sperling, B. A.; Calizo, I.; Cheng, G.; Hacker, C. A.; Zhang, Q.; Obeng, Y.; Peng, H. L.; Li, Q.; Zhu, X.; Yuan, H.; Walker, A. R. H.; Liu, Z.; Peng, L.; Richter, C. A. *ACS Nano* **2011**, *5*, 9144−9153.
(25) Nagashio, K.; Yamashita, T.; Nishimura, T.; Kita, K.; Toriumi, A. *J. Appl. Phys.* **2011**, *110*, 024513.
(26) Martins, A. B.; Schein, M. F.; Friedrich, J. L. R.; Fernandez-Lafuente, R.; Ayub, M. A. Z.; Rodrigues, R. C. *Ultrason. Sonochem.* **2013**, *20*, 1155−1160.
(27) Rokhina, E. V.; Lens, P.; Virkutyte, J. *Trends Biotechnol.* **2009**, *27*, 298−306.
(28) Belova, V.; Gorin, D. A.; Shchukin, D. G.; Mohwald, H. *ACS Appl. Mater. Interfaces* **2011**, *3*, 417−425.
(29) Young, T. *Philos. Trans. R. Soc. London* **1805**, *95*, 65.
(30) Yuan, L.; Dai, J.; Fan, X.; Song, T.; Tao, Y.; Wang, K.; Xu, Z.; Zhang, J.; Bai, X.; Lu, P.; Chen, J.; Zhou, J.; Wang, Z. *ACS Nano* **2011**, *5*, 4007−4013.
(31) Dresselhaus, M. S.; Jorio, A.; Hofmann, M.; Dresselhaus, G.; Saito, R. *Nano Lett.* **2010**, *10*, 751−758.
(32) Gui, L. L.; Yang, X.; Zhao, G. Z.; Yang, X.; Xiao, X. S.; Zhu, J. S.; Yang, C. X. *Appl. Opt.* **2011**, *50*, 110−115.